

1D MinION sequencing for large-scale species discovery: 7000 scuttle flies (Diptera: Phoridae) from one site in Kibale National Park (Uganda) revealed to belong to >650 species

Amrita Srivathsan¹, Emily Hartop^{2,5,6}, Jayanthi Puniamoorthy¹, Wan Ting Lee¹, Sujatha Narayanan Kutty^{1,4}, Olavi Kurina³, Rudolf Meier^{1,4*}

¹ Department of Biological Sciences, National University of Singapore, 14 Science Drive 4

² Zoology Department, Stockholms Universitet, Stockholm, Sweden

³ Estonian University of Life Sciences, Kreutzwaldi 5D, Tartu, Estonia

⁴ Tropical Marine Science Institute, National University of Singapore, Singapore

⁵ Station Linné, Öland, Sweden

⁶ Naturhistoriska Riksmuseet, Stockholm, Sweden

***Corresponding author:** Rudolf Meier: meier@nus.edu.sg

Other email addresses:

Amrita Srivathsan: asrivathsan@gmail.com

Emily Hartop: emhartop@gmail.com

Jayanthi Puniamoorthy: dbsjay@nus.edu.sg

Wan Ting Lee: dbslwt@nus.edu.sg

Sujatha Narayanan Kutty: tmssunk@nus.edu.sg

Olavi Kurina: Olavi.Kurina@emu.ee

Keywords: NGS barcoding, DNA barcoding, Nanopore sequencing, MinION, large-scale species discovery

1 **ABSTRACT**

2

3 Background: Most animal species remain to be discovered. We recently proposed to tackle this
4 problem using a 'reverse workflow' where all specimens are barcoded via tagged amplicon
5 sequencing and then sorted into putative species (mOTUs). We furthermore suggested that the
6 COI barcodes can be obtained with minimal laboratory equipment using MinION sequencing, but
7 our test with 1D² reads only yielded 500 barcodes per flowcell.

8

9 Results: Here we show how MinION 1D sequencing can be used to obtain ~3500 COI barcodes
10 per flowcell. Based on 7062 MinION barcodes for a hyper-diverse family of flies (Diptera:
11 Phoridae) collected by one trap in Kibale National Park, Uganda, we discover ~650 species which
12 exceeds the number of phorid species described for the entire Afrotropical region. Our updated
13 MinION pipeline increases processing speed via parallelization, improves demultiplexing, and yet
14 yields reliable barcodes (99.99% accuracy) and similar mOTUs as Illumina sequencing (match
15 ratio: 0.989). Morphological examination of 100 mOTUs confirms good congruence (93% of
16 mOTUs; >99% of specimens). Nearly 90% of species and specimens belong to the megadiverse
17 genus *Megaselia* which is routinely neglected because its species diversity and abundance is too
18 overwhelming. We show that it can be tackled with the reverse workflow. We also illustrate how
19 the molecular data guides the description of a new species: *Megaselia sepsioides* sp. nov..

20

21 Conclusions: MinION is suitable for reliable, rapid, and large-scale species discovery in
22 hyperdiverse taxa. Approximately 3500 specimens can be sequenced using one MinION flowcell
23 at a barcode cost of <0.35 USD.

24

25

26 INTRODUCTION

27 Most life on earth has yet to be discovered with an estimated 80% of extant species being still
28 unknown to science [1]. The majority of these species belong to hyper-diverse and species-rich
29 invertebrate clades. These taxa are ubiquitous, contain most of the multicellular animal species,
30 and often occur in great abundance. However, new species are difficult to find and delimit because
31 it requires the study of thousands of specimens. Typically, this process starts with sampling
32 specimens with bulk trapping methods (e.g. Malaise trap, fogging, pitfall traps, flight intercept
33 traps). It usually yields thousands of specimens per site that need to be sorted: first to higher-
34 level taxonomic groups by parataxonomists and then to species-level by taxonomic experts. The
35 latter work has to be carried out by taxonomic experts because species-level sorting by
36 parataxonomists tends to yield unreliable results [2]. Once morpho-species have been obtained,
37 they are then often tested via DNA barcodes (658 bp fragment of COI) by sequencing a few
38 representative specimens for each morpho-species [3]. This traditional workflow works well for
39 taxa with small numbers of species and specimens but is so time-consuming for hyperdiverse
40 and abundant clades that they are neglected. This is partially responsible for our lack of baseline
41 data for many insect taxa. The traditional workflow has the additional downside that
42 morphologically cryptic species are overlooked. This is particularly likely to happen when
43 expensive Sanger sequencing is used because only few specimens can be barcoded and the
44 probability of detecting cryptic species is low [4].

45

46 An alternative approach to species discovery is the 'reverse workflow' where every specimen in
47 a sample is individually sequenced (or barcoded) without the destruction of the specimen [4-6].
48 The specimens are then grouped to molecular Operational Taxonomic Units (mOTUs) based on
49 DNA barcodes. The morphological check of the putative species delimited with DNA barcodes
50 comes last. The taxonomic expert works on pre-sorted material and rectifies mis-sorted
51 specimens, identifies known species, and describes new species. This would have been deemed

52 unrealistically expensive prior to the advent of the High Throughput Sequencing technologies.
53 However, sequencing platforms like Illumina and PacBio are sufficiently cost-effective and are
54 now replacing barcoding via expensive Sanger sequencing [4, 5, 7-10]. For example, sequencing
55 tens of thousands of specimens with Illumina HiSeq can cost as little as 0.17 USD per specimen
56 (including PCR cost, see discussion in Wang et al., 2018 [4]). However, Illumina and PacBio
57 sequencing have some downsides. They are only cost-effective if >10,000 specimens have to be
58 barcoded, sequencing usually has to be outsourced (i.e., the amplicons have to be shipped to a
59 sequencing facility), and it often takes weeks to obtain data. It would be desirable to have
60 alternatives that are fast, scalable, and yet cost-effective. This would be particularly useful if
61 barcoding has to be accomplished under field conditions or in countries with limited access to
62 Illumina and PacBio sequencing [4, 5, 11, 12]. This is frequently the case and we therefore
63 strongly believe that the democratization of large-scale DNA barcoding will be important for
64 upscaling species discovery across the globe and encouraging the use of the reverse workflow
65 across many labs.

66

67 Oxford Nanopore's MinION has the potential to help with achieving these goals. It is a low-cost
68 and portable real-time sequencing device. However, its use and reliability for large scale
69 specimen handling remains to be fully understood. We recently showed that 500 reliable DNA
70 barcodes can be obtained using 1D² sequencing on one flowcell of MinION. To our knowledge
71 this was the highest number of products that were successfully multiplexed in a single MinION
72 flowcell (5X higher than a study which examined ~100 amplicons of rDNA [11]) but such low
73 throughput still meant that the cost per barcode remained high (ca. 2 USD: [13]). While this scale
74 is useful for many species' identification projects, it is unlikely to be effective for large-scale
75 species discovery where samples can contain thousands of specimens. Furthermore, the 500
76 specimens were barcoded using 1D² sequencing which requires a complicated library
77 preparation, base-calling is computationally intensive, and application to amplicon sequencing is

78 still under development. Unfortunately, it remained untested whether the more straightforward,
79 but less accurate 1D sequencing can be used for large-scale species discovery. This is addressed
80 in this manuscript.

81

82 However, we are here not only developing ways to use of MinION 1D sequencing for barcoding.
83 Instead, we are also investigating the curious observation that only 466 species of phorid flies
84 have been recorded for the Afrotropical Region [14]. Phoridae is a hyper-diverse clade belonging
85 to the true flies (Diptera). Diptera is one of several hyper-diverse insect orders that also include
86 beetles (Coleoptera), bees, wasps, and ants (Hymenoptera), and moths and butterflies
87 (Lepidoptera). The species estimates for all of Insecta vary between 3 and 13 million (reviewed
88 by Stork, 2018 [15]) with only ca. 1,000,000 currently being described [16]. Historically, the
89 *inordinate fondness* of taxonomists for beetles has led to Coleoptera outpacing Diptera and
90 Hymenoptera in numbers of described species. However, several recent studies suggest that
91 Hymenoptera and Diptera are likely to be more species-rich. For example, Forbes et al. [17]
92 hypothesize that Hymenoptera contained more species than either Diptera or Coleoptera based
93 on parasite host ratios for Microhymenoptera, but this study showed an underappreciation for
94 both the great numbers of Dipteran parasitoids and the diversity of true flies in general. Indeed,
95 Diptera has recently been proven to be surprisingly rich in a number of large-scale biodiversity
96 studies. In a large barcoding study of Canadian insects, Hebert et al. [18] found that Hymenoptera
97 and Diptera together accounted for two thirds of the 46,937 BINS acquired and predicted that one
98 dipteran family (Cecidomyiidae) has 16,000 species in Canada. The authors then extrapolated to
99 the worldwide fauna which they estimated to be 10 million insect species, of which 1.8 million
100 were predicted to be cecidomyiids [18]; i.e., a single family of Diptera may surpass the number of
101 described species in all of Coleoptera. Other studies similarly hint at the extraordinary richness of
102 Diptera. The Zurqui All Diptera Biodiversity Inventory (ZADBI) of a single site in Costa Rica was
103 heavily reliant on specimens collected with two Malaise traps run for a one-year period [19]. Only

104 41,001 specimens (a small fraction of the hundreds of thousands collected) could be studied by
105 taxonomic experts [20]. The specimens that were examined revealed 4,332 species of Diptera,
106 of which 800 were from Cecidomyiidae and 404 were for Phoridae [20], the fly family of focus
107 here.

108

109 Phoridae, or scuttle flies, are a worldwide family of true flies with approximately 4300 described
110 species [14]. Over 1600 of these are in the giant genus *Megaselia* Rondani, which has been
111 described as “one of the largest, most biologically diverse and taxonomically difficult genera in
112 the entire animal kingdom” [21]. In groups like *Megaselia*, the species discovery problem appears
113 insurmountable. Extremely large numbers of specimens are routinely collected, and they can
114 belong to very large numbers of species. Even in urban and suburban habitats, the diversity of
115 the family can be surprisingly high. Henry Disney, a world expert on the family, has recorded 75
116 species of phorids (48 of *Megaselia*) in his modest suburban garden [22]. Similarly, the BioSCAN
117 project in Los Angeles found that backyards in the city supported as many as 82 species [22]. In
118 natural areas, the diversity and abundance tend to be much higher and sorting such samples into
119 species-level units using traditional workflows is very labor-intensive. Rare and new species are
120 often hidden among very large numbers of common and described species. The study of groups
121 like *Megaselia* requires examination of thousands of specimens for which prodigious notes have
122 to be taken as specimens are compared. Many detailed drawings are prepared (for *Megaselia*
123 drawings of male genitalia are essential) – often based on dissections and slide mounts – because
124 many known/common species cannot be identified without detailed inspection. The process can
125 take hours, days, or longer for a single species discovery. This traditional workflow thus often
126 discourages all but the most tenacious taxonomists from taking up the study of hyper-diverse
127 genera within insects.

128

129 Here, we test whether 1D MinION sequencing may offer a rapid and revolutionary approach to
130 exploring phorid diversity more comprehensively. MinION sequencing is here applied to ca. 30%
131 of the phorid specimens that were collected in a single Malaise trap in Kibale National Park,
132 Uganda. We here describe how we processed ~8700 specimens, obtained ~7000 accurate
133 barcodes, and found 650 species (of which almost 90% are *Megaselia*). All this could be
134 accomplished using a workflow that requires less than a month.

135

136 **RESULTS**

137 **MinION based DNA barcoding**

138 The experiment was designed to obtain full-length COI barcodes for two sets of specimens via
139 tagged amplicon sequencing. A total of 8699 specimens were processed (Set 1: 4275; Set 2:
140 4519; 95 specimens were shared between the sets) (Fig. 1). In order to assess amplification
141 success rates, a subset of PCR products for each of the ninety-two 96-well plates were assessed
142 with agarose gels. The extrapolated amplification success rates were 86% and 74% for the two
143 sets of specimens (80.7% overall); i.e., we estimated that >3600 and >3300 DNA barcodes should
144 be obtainable via MinION sequencing given that gels tend to underestimate amplification success
145 rates (Table 1). The PCR products for each set were pooled and sequenced using MinION (set
146 1: 7,035,075; set 2: 7,179,121 1D nanopore reads). Both sets were sequenced in two sequencing
147 runs. The first run for each set was based on the pooled PCR products for all specimens in the
148 sets. It generated 3,069,048 and 4,853,363 reads, respectively. The results of the first run were
149 used to estimate coverage for each PCR product. Products with weak coverage ($\leq 50x$) were re-
150 pooled and re-sequenced (set 1: 2172 amplicons; set 2: 2211 amplicons). This added 3,966,027
151 and 2,325,758 reads to each set and improved the coverage of many low-coverage barcodes
152 (Fig. 2). The combined data were processed using an improved version of the bioinformatics
153 pipeline in Srivathsan et al. [13]. The improvements led to a higher demultiplexing rate (14%

154 increase for set 1: 898,979 vs. 787,239 reads; 9% increase for set 2: 647,152 vs. 593,131 reads)
155 and faster demultiplexing (10X using 4 cores: demultiplexing in 9 min vs 87 min for one of the
156 datasets).

157 Demultiplexing of all data and preliminary barcode calling revealed 3,797 and 3,476 MAFFT
158 barcodes with $\geq 5X$ coverage and $< 1\%$ ambiguous bases. These barcodes were subject to
159 correction using RACON [23] which yielded the same number of barcodes. When the barcodes
160 for the two sets of samples were combined, we overall obtained 7,220 MAFFT and RACON
161 barcodes. These preliminary barcodes still contain indel and substitution errors that were
162 addressed with an amino-acid correction pipeline that was first implemented in Srivathsan et al.
163 [13]. It yielded 7,178 MAFFT+AA and 7,194 RACON+AA barcodes. Some barcodes were not
164 retained because this pipeline rejects barcodes that have five or more consecutive indel errors.
165 Finally, the two sets of corrected barcodes were consolidated. This yielded a set of 7,115
166 consolidated barcodes. We rejected barcodes where the alignment of MAFFT+AA and
167 RACON+AA barcodes required the insertion of indels, as the +AA barcodes are expected to be
168 indel-free. Such indels in the alignments of MAFFT+AA and RACON+AA barcodes also indicate
169 discrepancies between MAFFT and RACON barcode estimates and there is no objective reason
170 to prefer one barcode over the other. The overall barcoding success rate was thus 81.9% (7,115
171 barcodes for 8,699 specimens). This was close to the expected 80.7% success rate based on gel
172 electrophoresis; i.e., MinION sequencing consistently produced sequence data for successfully
173 amplified products. A subsequent contamination check via BLAST revealed that of the 7,115
174 barcodes, 53 barcodes were unlikely to pertain to phorid flies ($< 1\%$) and we thus retained 7,062
175 barcodes for species richness estimation. Lastly, we inspected the reads obtained for the 92
176 negative controls (1 per microplate). Five negatives yielded MAFFT barcodes. Four of these had
177 a $> 97\%$ match to non-phorids (two humans, one fish, one mollusc) and were eliminated. One low
178 coverage (13X) negative survived all filters and matched phorid COI. It was removed after

179 ascertaining that it did not impact the accuracy of the barcodes in the plate. This could be tested
180 by comparing the MinION barcodes for the plate with Illumina barcodes obtained from different
181 PCR products for the same DNA extraction plate (see below).

182 **Accuracy and selection of barcode sets**

183 To find the best strategy for obtaining accurate barcodes, we compared 5 sets of barcodes
184 (MAFFT, RACON, MAFFT+AA, RACON+AA, and consolidated barcodes) with the corresponding
185 barcodes based on Illumina sequencing. Illumina barcodes were obtained for 6,373 specimens
186 for the same specimens using different primers that amplified a 313 bp subset of the full-length
187 barcodes. The comparisons showed that the uncorrected MAFFT and RACON barcodes had an
188 accuracy of 99.61% and 99.51% (Table 2). Correction of these barcodes using the amino-acid
189 correction pipeline improved the accuracy considerably (>99.9% in all cases). The barcodes were
190 corrected after testing several “namino” parameters. Overall, namino=2 was found to yield the
191 most accurate barcodes, and minimized the number of inaccurate barcodes. We found that
192 MAFFT+AA barcodes were more accurate than RACON+AA barcodes, but MAFFT+AA barcodes
193 contained a much higher number of ambiguous nucleotides (Fig. 3). When RACON+AA and
194 MAFFT+AA barcodes were consolidated, the resulting “consolidated barcodes” were found to be
195 highly accurate (99.99%) and contained few ambiguous bases (median = 0.3 %).

196 We furthermore compared the mOTU richness estimated by the different barcode sets. mOTU
197 richness was very similar across MinION and Illumina barcodes for the consolidated and
198 uncorrected MAFFT/RACON barcodes. MAFFT+AA barcodes performed well in this comparison,
199 but yielded fewer mOTUs than Illumina barcodes: this may be due to a higher proportion of
200 ambiguous nucleotides (Fig. 3). However, comparison of mOTU richness alone does not imply
201 the same specimens were grouped into mOTUs across MinION and Illumina barcode sets. We
202 thus also calculated the match ratio for the datasets (3% clustering threshold). We found that all
203 five barcode sets (MAFFT, RACON, MAFFT+AA, RACON+AA, and consolidated barcodes,

204 namino=2) also had high match ratios (>0.97) with the consolidated barcodes and RACON
205 barcodes performing best with match ratios of >0.98 (consolidated barcodes: 0.989, RACON:
206 0.989, RACON+AA: 0.982). However, upon closer inspection only the multiple sequence
207 alignment (MSA) of the consolidated barcodes was indel-free while the other MSAs contained
208 indels. The largest number of indels was found in the MSA of uncorrected RACON barcodes
209 which indicates that the RACON barcodes retain a fair number of indels and may not be of
210 sufficient quality for submission to sequence databases. Overall, we would thus recommend the
211 usage of consolidated barcodes as the final barcode set. Because they maximize the per-base
212 accuracy, estimated mOTU diversity, match ratios, and yield high-quality alignments.

213 **Species richness estimation**

214 We thus proceeded to characterize the diversity of the phorid flies collected from the Malaise traps
215 based on the consolidated barcodes (namino=2). We overall obtained a mean of 683 mOTUs
216 (2%: 728, 3%: 685, 4%: 636) when the thresholds were varied from 2-4%. Species accumulation
217 and Chao 1 curves for mOTUs at 3% were not found to have reached a plateau, but the shape of
218 the curves suggest an estimated diversity is >1000 species in a single site collected by one
219 Malaise trap (Fig. 4).

220 **Congruence with morphology**

221 mOTUs are expected to be affected by mistakes caused by lab contamination and species
222 delimitation errors due to the biological properties of barcodes. We find that 6 of the 100 clusters
223 contained a single misplaced specimen and that there was one small cluster of four specimens
224 that appeared to consist of a mixture three morpho-species. This implies that 9 of the >1500
225 examined barcoded specimens were misplaced due to lab contamination. mOTUs based on
226 barcodes are expected to underestimate species for those that recently speciated and
227 overestimate species with deep splits [24]. This means that taxonomists working with mOTUs

228 should check for signs of lumping and splitting for closely related taxa. Our initial morphological
229 check of 100 randomly selected clusters (>1500 specimens) took ca. 30 hours. This preliminary
230 morphological screening covered all specimens while future studies could concentrate on
231 complex clusters, as any differences that may have occurred within 5% clusters were not
232 discernible without further preparations (dissection and slide mounting). Identifying these areas
233 of potential ambiguity is an advantage of this pipeline. It allows taxonomic experts to focus time
234 and energy on these complex clusters.

235

236 **New Species Description**

237

238 A primary aim of the reverse workflow is finding rare new species for description in bulk samples.
239 With specimens pre-sorted into mOTUs, morphologists have easy access to interesting and
240 potentially rare species that would otherwise remain undiscovered. While examining the 100
241 mOTUs, eight specimens were found to belong to a distinctive new species of *Megaselia*. This
242 species provided a good opportunity to demonstrate how the reverse workflow aids in species
243 discovery because a mOTU-specific haplotype network informed on which specimens should be
244 studied with morphology. The species is here described, and the description incorporates the
245 molecular data.

246

247 *Megaselia sepsioides* Hartop sp. n.

248 urn:lsid:zoobank.org:pub:ED268DF2-A886-4C31-A4FB-6271C382DECE

249

250 **Description**

251 See Fig. 5, 6.

252 In an effort to continue reducing redundancy and ambiguity in species descriptions, the
253 description of this species has excluded the character table from the method previously
254 established for *Megaselia* [25-27] and uses a barcode and photographic description. Photographs
255 are a key element in descriptions for large, diverse groups [28], where verbose descriptions can
256 be both overwhelmingly time consuming and insufficiently diagnostic. Most characters that would
257 have been in table form are clearly visible in the photographs provided; the few that are not were
258 deemed irrelevant to either the description or diagnosis of the species.

259

260 **Diagnosis**

261 This species is unmistakable even within the gargantuan and taxonomically difficult
262 genus *Megaselia*. The semi-circular expansion with modified peg-like setae on the forefemur is
263 unique among described members of the genus (Fig. 5, b). Similarly, the severe constriction of
264 the hind tibia basally is diagnostic (Fig. 5, d and e). The narrow and elongate form of the abdomen
265 is notable. Fig. 6 shows variations in setation between haplotypes. Only single specimens of the
266 two distinct haplotypes are available; more specimens will be necessary to determine if these are
267 eventually removed as distinct species or fall within a continuum of intraspecific variation.

268 DNA barcode for UGC0005996:

269 actttatatttttttgagcttgagctggaatagtaggtacttcctaagaatcataattcgtgctgaattaggacaccaggagcacttat
270 tggatgaccaaattataatgtgattgttactgcacatgctttattataatTTTTTatagtaaacctattataataggaggtttggaattg
271 acttgtaaccttaataataggagccccagatatggcattccctcgaatgaataatataagTTTTTgaatattacctcctcttaactctttatta
272 gccagaagtatagtagaaaatggagctggaactggtgaacagttatcctccttatctctagaatcgctcatagtgagcttctgtgat
273 ttagcaattttctctctcatttagctggaattcatctatttaggagctgtaaattttattacaacaattattaatatacgatcatcaggtattaca
274 ttgaccgaataacctctattgtttgatctgtaggtattacagctttattgctactcttatcactcctgTTTTtagctggtgctattacaatactattaa
275 cagaccgaaatttaataacttcatttttgaccagcaggaggagatccaattttataccaacatttttc

276

277 **Material Examined**

278

279 Holotype:

280 Scientific Name: *Megaselia sepsioides* Hartop 2019; country: Uganda; state Province:
281 Kamwenge; locality: Kibale National Park: 1530 m; Coordinates: 00°33'54.2"N 30°21'31.3"E;
282 sampling protocol: Malaise trap; event date: iii-xii, 2010; individual count: 1; sex: male; life stage:
283 adult: UGC0005996; identified by: Emily Hartop: 2019; institution code: LKCNHM; collection code:
284 UGC; basis of record: preserved specimen.

285

286 Paratypes:

287 Scientific name: *Megaselia sepsioides* Hartop 2019; country: Uganda; state province:
288 Kamwenge; locality: Kibale National Park; elevation: 1530 m; coordinates: 00°33'54.2"N
289 30°21'31.3"E; sampling protocol: Malaise trap; event date: iii-xii, 2010; individual count: 7; sex:
290 male; life stage: adult; catalog number: UGC0012899, UGC0012244, UGC0012568,
291 UGC0003003, UGC0005864, UGC0012937, UGC0012971; identified by: Emily Hartop; date
292 identified: 2019; institution code: LKCNHM; collection code: UGC; basis of record: preserved
293 specimen

294

295 **Distribution**

296 Known from a single site in Kibale National Park, Uganda.

297

298 **Biology**

299 Unknown.

300

301 **Etymology**

302 Named by Yuchen Ang for the sepsid-like (Diptera: Sepsidae) foreleg modification.

303

304 **DISCUSSION**

305

306 *Large scale species discovery using MinION*

307

308 Our results suggest that MinION's 1D sequencing yields data of sufficient quality for producing
309 high-quality DNA barcodes that can be used for large-scale species discovery. Through the
310 development of new primer-tags, sequencing strategies, and improved bioinformatics
311 procedures, we here increase the barcoding capacity of a MinION flowcell from 500 specimens
312 (Srivathsan et al., 2018: 1D² sequencing) to ~3500 specimens. This is achieved without a drop in
313 accuracy because the new error correction pipeline is effective at eliminating most of the errors
314 in the 1D reads (ca. 10%). Indeed, even the initial MinION barcodes (MAFFT & RACON) have
315 very high accuracy (>99.5%) when compared to Illumina data. Note that this accuracy is even
316 higher than what was obtained with 1D² sequencing in Srivathsan et al. (2018: 99.2%). We
317 suspect that this partially due to improvements in MinION sequencing chemistry and base-calling,
318 but our upgraded bioinformatics pipeline also helps because it increases coverage for the
319 amplicons. These findings are welcome news because 1D library preparations are much simpler
320 than the library preps for 1D². In addition, 1D² reads are currently less suitable for amplicon
321 sequencing (<https://store.nanoporetech.com/kits-250/1d-sequencing-kit.html>) [29].

322

323 We tested a range of different techniques for obtaining barcodes from 1D reads. Some techniques
324 are computationally more expensive than others which raises the question of which bioinformatics
325 pipeline should be used for obtaining accurate barcodes. Based on the current performance of
326 MinION, we would recommend the usage of the "consolidated barcodes". They contain no indel
327 errors and fewer substitution errors (99.99% accuracy) when compared to MAFFT+AA and
328 RACON+AA barcodes. The mOTUs delimited with consolidated barcodes are virtually identical
329 with the ones obtained via Illumina sequencing (Number of 3% mOTUs for Illumina: 661; MinION:

330 658; match-ratio: 0.989). In addition, consolidated barcodes were also the most accurate
331 barcodes based on 1D² reads [13]. Nevertheless, we found that all barcode sets gave reliable
332 mOTU estimates. For corrected barcodes (MAFFT+AA and RACON+AA) this was consistent with
333 >99.9% per base accuracy, but the higher error rates of the uncorrected barcodes rarely affected
334 mOTU estimates. This is because indels were treated as missing data and mOTU estimation only
335 requires accurate estimates of distances for closely related taxa. This explains why the 99.5%
336 accurate RACON barcodes can group specimens into mOTUs in a very similar manner to what
337 is obtained with Illumina barcodes (match ratio of >0.98). The results imply that accurate mOTU
338 estimates can be obtained even based on preliminary barcodes.

339

340 Based on the procedures described here, MinION barcodes can be generated rapidly and at a
341 low sequencing cost of <0.35 USD per barcode. These properties make MinION a valuable tool
342 for species discovery whenever a few thousand specimens have to be sorted to species (<5000).
343 Even larger-scale barcoding is probably still best tackled with Illumina short-read or PacBio's
344 Sequel sequencing [4, 5, 7] because the cost is lower and the quality of the reads is higher.
345 However, both require access to expensive sequencers, the sequencing has to be outsourced,
346 and the users usually have to wait for several weeks in order to obtain the data. This is not the
347 case for barcoding with MinION where most of the data are collected within 10 hours of
348 sequencing. Our proposed MinION pipeline has the additional advantage that it only requires
349 basic molecular lab equipment including thermocyclers, magnetic rack, Qubit and potentially a
350 server computer. The latter is only needed for base-calling and should be replaceable by a new
351 portable, custom-built computational device for base-calling ONT data ("MinIT") while
352 demultiplexing and barcode-calling only requires a regular laptop computer. Overall, these
353 requirements are minimal which means that fully functional barcoding labs can be established for
354 <USD 5,000. Arguably, the biggest operational issue may be access to a sufficiently large number

355 of thermocyclers given that a study of the scale described here involved amplifying PCR products
356 in 92 microplates (=92 PCR runs).

357

358 Our new workflow for large-scale species discovery is based on sequencing the amplicons in two
359 sequencing runs. The second sequencing run can re-use the flowcell that was used for the first
360 run. Two runs are desirable because it improves overall barcoding success rates. The first run is
361 used to identify those PCR products with “weak” signal (=low coverage). These weak products
362 can then be re-sequenced in the second run. This dual-run strategy is designed to overcome the
363 challenges related to sequencing large numbers of PCR products: the quality and quantity of DNA
364 extracts are poorly controlled and PCR efficiency varies considerably. Pooling of products ideally
365 requires normalization, but this is not practical when thousands of samples are handled. Instead,
366 one can use the real-time sequencing provided by MinION to determine coverage and then boost
367 the coverage of low-coverage products by preparing and re-sequencing a separate library that
368 contains only the low coverage samples. Given that library preparations only require <200 ng of
369 DNA, even a set of weak amplicons will yield a sufficient amount of DNA.

370

371 *MinION sequencing and the “reverse workflow”*

372

373 Based on our data, we would argue that MinION is now suitable for implementing the “reverse-
374 workflow” where all specimens are sequenced first before mOTUs are assessed for morphological
375 consistency. This differs from the traditional workflow in that the latter requires sorting based on
376 morphology with only some morpho-species being subsequently tested via limited barcoding. We
377 would argue that the reverse-workflow is more suitable for handling species- and specimen-rich
378 clades because it requires less time than high-quality sorting based on morphology which often
379 involves genitalia preparations and slide-mounts. We would argue that expert sorting and

380 identification of material based on morphology is only very efficient for taxa where species-specific
381 morphological characters are easily accessible and the number of specimens is small. However,
382 most undiscovered and undescribed species are in poorly explored groups and regions where
383 specimen sorting and identification using the traditional techniques will be much slower. For
384 example, even if we assume that an expert can sort and identify 50 specimens of unknown phorids
385 per day, the reverse workflow pipeline would increase the species-level sorting rate by >10 times
386 (based on the extraction and PCR of six microplates per day). In addition, the sorting would be
387 carried out by lab personnel trained in amplicon sequencing while accurate morpho-species
388 sorting requires highly specialized taxonomic experts. Even such highly trained taxonomic experts
389 are often not able to match males and females of the same species (often one sex is ignored in
390 morphological sorting) while the matching of sexes and immatures is an automatic and desirable
391 byproduct of applying the reverse workflow [6].

392

393 One key element of the reverse workflow is that vials with specimens that have haplotype
394 distances <5% are physically kept together. This helps when taxonomic experts scrutinize
395 mOTUs for congruence with morpho-species. Indeed, graphical representation of haplotype
396 relationships (e.g., haplotype networks) can be used to guide morphological re-examination as
397 illustrated in our description of *Megaselia sepsioides* (Fig. 7). The eight specimens belonged to
398 seven haplotypes, the most distant haplotypes were dissected in order to test whether the data
399 are consistent with one or two species. Variations in setation were observed (Fig. 6) that were
400 deemed likely to be consistent with intraspecific variation. Note that the morphological
401 examination of clusters is straightforward because the use of QuickExtract for DNA extractions
402 ensures morphologically intact specimens. We predict that taxa that have been historically
403 ignored or understudied due to extreme abundance of common species and high species diversity
404 will now become more accessible because taxonomic experts can work on pre-sorted material
405 instead of thousands of unsorted specimens.

406

407 But how good is the correspondence between mOTUs and morpho-species. We checked 100
408 randomly chosen mOTUs for congruence with morphospecies. We find that 93% of clusters are
409 congruent, and over 99% of specimens (six of the seven cases of incongruence were single
410 specimens). This is in line with congruence levels that we observed for ants and odonates [4, 6].
411 This means that MinION barcodes are not only reliable but also yield mOTUs that are largely
412 congruent with morphospecies. This also means they are suitable for characterizing even
413 complex and species-rich samples of hyper-diverse invertebrate clades.

414

415 *Remarkably high diversity of Phoridae in Kibale National Park*

416 It is astonishing that the barcodes obtained from a single site in Kibale National Park (Uganda)
417 revealed ca. 650 mOTUs of phorid flies. This diversity, obtained from one Malaise trap, contains
418 150% of the number of described phorid species (466) known from the entire Afrotropical region;
419 i.e., numerically at least 184 species must be new to the region or to science [14]. Note that the
420 barcoded specimens only represent 8 one-week samples between March 2010 and February
421 2011; i.e., forty-four samples obtained from the same Malaise trap remain un-sequenced. We
422 thus expect the diversity from this single site to eventually well exceed 1000 species (Fig. 4).

423

424 The unexpectedly high species richness found in this study inspired us to muse about the species
425 diversity of phorids in the Afrotropical region. This is what Terry Erwin did when he famously
426 estimated a tropical arthropod fauna of 30 million species based on his explorations of beetle
427 diversity in Panama [30]. Such speculation is useful because it raises new questions, inspires
428 follow-up research, and may be needed given that even with extensive sampling, the species
429 richness of diverse taxa can be remarkably difficult to estimate [31]. The Afrotropical region
430 comprises roughly 2000 squares of 100 km² size. In our study we only sampled a tiny area within

431 one of these squares and observed 650 species which are likely to represent a species
432 assemblage that exceeds >1000 species. This will only be a subset of the phorid fauna in the
433 area because many specialist species (e.g., termite inquilines) are not collected in Malaise traps.
434 Of course, the 1000 species are also only a subset of the species occurring in the remaining
435 habitats in the same 100 km² square which is likely to be home to several thousand species of
436 phorids. But let's only assume that on average each of the two-thousand 100 km² squares have
437 100 endemic phorid species. If so, the "endemic" phorids alone would contribute 200,000 species
438 of phorids to the Afrotropical fauna without even considering the contributions to species diversity
439 by the "normal" species turnover of the remaining species. These considerations make us believe
440 that it would be somewhat surprising if the Afrotropical region were to have fewer than half a
441 million species of phorids! Based on our sample from Kibale National Park, 90% of species and
442 specimens would belong to *Megaselia* as currently circumscribed. Could it be that there are
443 450,000 species of Afrotropical *Megaselia*? These guesstimates would only be much lower if the
444 vast majority of phorid species had very wide distributions which we consider somewhat unlikely
445 given that the Afrotropical region covers a wide variety of climates and habitats.

446

447 As documented by our study, the bulk of phorid species are *Megaselia*. Based on the traditional
448 workflow, almost all these specimens would be relegated to unsorted Malaise trap residues for
449 decades or centuries. Indeed, there are thousands of vials labeled as "Phoridae" decorating the
450 shelves of all major museums worldwide. The traditional workflow is not able to keep pace with
451 the species numbers and abundance. This makes rapid species-level sorting with "NGS
452 barcodes" [4] so important. Biologists will finally be able to work on taxa that are so specimen-
453 and species-rich that they were considered unworkable with the traditional techniques. MinION
454 barcodes will be one of the techniques that can be used to tackle these clades. We predict that
455 these barcodes will become particularly important for setting up mobile laboratories that can

456 operate under field conditions, but MinION barcodes can also be generated by highschool
457 students and citizen scientists.

458

459 **METHODS**

460 **1. Sampling**

461 Samples were collected from a single Townes-type Malaise trap [32], in the Kibale National Park,
462 close to Kanyawara Biological Station in the evergreen primeval forest at an altitude of 1513 m
463 (00°33'54.2"N 30°21'31.3"E) (Fig. 4). Kibale National Park is characterized as a fragment of
464 submontane equatorial woodland being home to 216 tree species [33]. Temperatures in Kibale
465 range from 16°C to 23°C (annual mean daily minimum and maximum, respectively) [34]. As
466 described, the Malaise trap was checked every week when the collecting bottle with the material
467 was replaced by a resident parataxonomist ([35]: Mr. Swaibu Katusabe). The material in Kibale
468 National Park in Uganda was collected and transferred in accordance with approvals from the
469 Uganda Wildlife Authority (UWA/FOD/33/02) and Uganda National Council for Science and
470 Technology (NS 290/ September 8, 2011), respectively. The material was thereafter sorted to
471 higher-level taxa. Target Diptera taxa were sorted to family and we here used Phoridae. The
472 sampling was done over several months between 2010 and 2011. For the study carried out here,
473 we only barcoded ca. 30% of the phorid specimens. The flies were stored in ethyl alcohol at -20–
474 25°C until extraction.

475 **2. DNA extraction**

476 DNA was extracted using 10 ul of QuickExtract in a 96 well plate format and the whole fly was
477 used to extract DNA. The solution with the fly was incubated at 65°C for 15 min followed by 98°C
478 for 2 min. No homogenization was carried to ensure that intact specimen was available for
479 morphological examination.

480

481 **3. MinION based DNA barcoding**

482

483 *I. Polymerase Chain Reactions (PCRs)*

484 Each plate with 96 QuickExtract extracts (95 specimens and 1 control, with exception of one plate
485 with no negative and one partial plate) was subjected to PCR in order to amplify the 658 bp
486 fragment of COI using LCO1490 5' GGTCACAAATCATAAAGATATTGG 3' and HCO2198 5'
487 TAAACTTCAGGGTGACCAAAAAATCA 3' [36]. Each PCR product was amplified using primers
488 that included a 13 bp tag. For this study, 96 thirteen-bp tags were newly generated in order to
489 allow for upscaling of barcoding; these tags allow for multiplexing >9200 products in a single
490 flowcell of MinION through unique tag combinations (96x96 combinations). To obtain these 96
491 tags, we first generated one thousand tags that differed by at least 6 bp using with
492 BarcodeGenerator (http://comailab.genomecenter.ucdavis.edu/index.php/Barcode_generator)
493 [37] However, tag distances of >6 bp are not sufficient because they do not take into account
494 MinION's propensity for generating homopolymer and other indel errors. We thus excluded tags
495 with homopolymeric stretches that were >2 bp long. We next used a custom script that identified
496 tags that differed from each other by indel errors and eliminated tags recursively to ensure that
497 the final sets of tags differed from each other by >=3bp errors of any type (any combination of
498 insertions/deletions/substitutions). This corresponded with our bioinformatic strategy of using
499 <=2bp mismatch in tag identification. Lastly, we excluded tags that ended with "GG" because
500 LCO1490 starts with this motif. The PCR conditions were as follows, reaction mix: 10 µl Mastermix
501 from CWBio, 0.16 µl of 25mM MgCl₂, 2 µl of 1 mg/ml BSA, 1 µl each of 10 µM primers, and 1ul of
502 DNA. The PCR conditions were 5 min initial denaturation at 94°C followed by 35 cycles of
503 denaturation at 94°C (30 sec), 45°C (1 min), 72°C (1 min), followed by final extension of 72°C
504 (5min). For each plate, a subset of 7-12 products were run on a 2% agarose gel to ensure that
505 PCRs were successful. Of the 96 plates studied, 4 plates were excluded from further analyses as

506 they had <50% amplification success and one plate was duplicated across the two runs by
507 accident.

508

509 *II. MinION sequencing*

510 The most cost-effective strategy for nanopore sequencing was optimized during the study. For
511 the initial experiment (set 1) we sequenced amplicons for 4275 phorid flies. The flowcell was used
512 for 48 hours and yielded barcodes for ~3200 products, but we noticed lack of data for products
513 for which amplification bands could be observed on the agarose gel. We thus re-pooled all
514 products with a sequencing depth $\leq 50X$ (2119 specimens), prepared a new library and
515 sequenced them on a new flowcell. The experiment was successful. However, in order reduce
516 sequencing cost, we pursued a different strategy for the second set of specimens. This set
517 consisted of pooled amplicons for 4519 flies, but here we stopped the sequencing on the flowcell
518 after 24 hours. The flowcell was then washed using ONT's flowcell wash kit and prepared for
519 reuse. The results from the first 24 hours of sequencing were used to identify amplicons with weak
520 coverage. They were re-pooled, a second library was prepared, and sequenced on the pre-used
521 and washed flowcell.

522

523 Amplicon pooling strategy: For set 1, all plates were grouped by amplicon strength as judged by
524 the intensity of products on agarose gels (5 strong pools +2 weak pools). For set 2, each plate
525 was pooled, quantified, and cleaned using either 1X Ampure beads or 1.1X Sera-Mag beads in
526 PEG. For the re-sequencing of weak or "problematic" products (see below), we identified the latter
527 based on the results of the initial sequencing run. We located (1) specimens $\leq 10X$ coverage (set
528 1: 1054, set 2: 1054) and (2) samples with coverage between 10X and 50X (set 1: 1118, set 2:
529 1065). Lastly, we also created a (3) third pool of specimens with problematic products that were
530 defined as those that were found to be of low accuracy during comparisons with Illumina barcodes
531 and those that had high levels of ambiguous bases ($>1\%$ ambiguous bases during preliminary

532 barcode calling). Very few amplicons belonged to this category (set 1: 68, set 2: 92) and it is thus
533 not included in the flowchart in Figure 1. In order to efficiently re-pool hundreds of specimens
534 across plates we wrote a script that generates visual maps of the all microplates that illustrate
535 where the weak products are found.

536
537 Library preparation and sequencing: We used the SQK-LSK109 ligation sequencing kit for library
538 preparation and sequencing. Our first experiment on set 1 used 1 ug of starting DNA while all
539 other libraries used 200 ng pooled product. Library preparation was carried out as per
540 manufacturer's instructions with one exception: the various clean-up procedures at the end-prep
541 and ligation stages used 1X Ampure beads instead of 0.4 X as suggested in the instructions
542 because the amplicons in our experiments were short (~735 bp with primers and tags). The
543 sequencing was carried out using MinION sequencer with varying MinKNOW versions between
544 August 2018 - January 2019. Fast5 files generated were uploaded onto a computer server and
545 base-calling was carried out using Guppy 2.3.5+53a111f. No quality filtering criteria were used.
546 Our initial work with Albacore suggested that quality filtering improved demultiplexing rate but
547 overall more reads could be demultiplexed without the filtering criterion.

548
549 *III. Data analyses for MinION barcoding*

550 We analysed the data using miniBarcoder [13], which was improved in several ways for the
551 present study. Overall, the pipeline starts with a primer search with *glsearch36*, then flanking
552 nucleotide sequences are identified, and reads are demultiplexed based on tags. For the latter,
553 an error of up to 2 bp errors are allowed. The demultiplexed reads are aligned using MAFFT v7
554 (--op 0) (here v7) [38]. In order to improve speed, we used only a random subset of 100 reads
555 from each demultiplexed file for alignment. Based on these alignments, a majority rule consensus
556 is called to obtain what we call "MAFFT barcodes". A second preliminary barcode is generated
557 by mapping all reads back to the MAFFT barcode using Graphmap (here v0.5.2) [39] and calling

558 the consensus using Racon (here, v1.3.1) [40]. This yields what we call “RACON barcodes”. Both
559 MAFFT and RACON barcodes are subject to further correction based on publicly available
560 barcodes in GenBank. These corrections are advisable in order to fix remaining indel errors. The
561 correction takes advantage of the fact that COI sequences are translatable; i.e., an amino-acid
562 based error correction pipeline can be used (details can be found in Srivathsan et al. (2018)).
563 Applying this pipeline to MAFFT and RACON barcodes respectively yields MAFFT+AA and
564 RACON+AA barcodes. Lastly, these barcodes can be consolidated by comparing them to yield
565 “consolidated barcodes”.

566

567 The version of the pipeline in Srivathsan et al. [13] was modified as follows:

568

569 *a. Tackling 1D reads for massively multiplexed data:* The large number of simultaneously
570 barcoded specimens presented many challenges related to varying coverage and quality. We
571 hence sought to develop ways to account for increased error rates of 1D sequencing and develop
572 objective ways for quality assessments based on the MinION data and publically available data
573 (GenBank): (1) The GraphMap max error was increased from 0.05 to 0.15 to account for error
574 rates of 1D reads. (2) We modified the approach for calculating consolidated barcodes. We here
575 use the strict consensus of MAFFT+AA and RACON+AA barcodes in order to resolve conflicts
576 between MAFFT and RACON barcodes if there are substitution conflicts. In Srivathsan et al.
577 (2018) we accepted MAFFT+AA barcodes in cases of conflict, but for the 1D data we found that
578 MAFFT+AA barcodes had more ambiguities than RACON+AA barcodes which could be resolved
579 via calculating a strict consensus. We also introduced a criterion for identifying “problematic”
580 barcodes based on observing too many differences between MAFFT+AA and RACON+AA
581 barcodes; i.e., if indels are found in the alignment of MAFFT+AA and RACON+AA barcode during
582 consolidation, the barcode is rejected. This criterion is based on the fact that +AA barcodes should
583 be indel-free. Either the MAFFT+AA or the RACON+AA barcode is likely to be incorrect, but there

584 is no objective way to identify the correct sequence. (3) We assessed how different window sizes
585 can impact the amino-acid correction pipeline by varying the “namino” parameter (number of AA
586 to be inspected in each side of an indel).

587

588 *b. Demultiplexing rate:* (1) We introduced a “homopolymer compression” of the putative tag
589 sequences in order to improve demultiplexing rates. After primer searches, the old pipeline used
590 to identify the flanking 13 bps that were likely to be tag sequence. Instead we now use a 20 bp
591 flanking sequence and then compress any homopolymer >3bp before searching for 13 bp tags.

592 (2) We now analyze reads that are likely the result of two products that ligated during library
593 preparation. This was based on our experience with one library where ligation of products was
594 prominent. Long reads are split into size classes of <1300, >1300 and <2000. These settings
595 were set based on 658 bp barcode of COI: the total product size including tags and primers is
596 735 bp, and hence, a sequence with two products ligated to each other is expected to be 1470
597 bp long. The sequences were split in a manner that ensured that the tags of first product are not
598 affecting the tag found in the second, i.e., primer search for second product was conducted after
599 the first 650 bp of the sequence. Currently, this option is only available for reads that consist of
600 two ligated products.

601

602 *c. Processing speed and memory requirements:* (1) For primer identification we now limit the
603 searches to the first and last 100 bp of each read which allowed for improving speed of the primer
604 search. (2) We parallelized the process of demultiplexing and MAFFT barcode calling using
605 multiprocessing in python. This allows for fast demultiplexing whenever computational power is
606 limited. (3) We optimized the pipeline with regard to memory consumption and ensured that all
607 processes are applied to batches of ≤ 20000 sequences. The latter modification is needed given
608 the rapid increase in MinION output and batch processing is scalable with increased output.

609

610 **4. Illumina Based NGS Barcoding for validation**

611 In order to validate MinION barcodes and optimizing error correction strategies, we used
612 reference COI barcodes obtained via Illumina sequencing for the same QuickExtract DNA
613 extractions. Illumina sequencing was carried out for a 313 bp fragment of the same COI barcoding
614 region using m1COLintF: 5'-GGWACWGGWTGAACWGTWTAYCCYCC-3' [41] and modified
615 jgHCO2198: 50-TANACYTCNGGRTGNCCRAARAA YCA-3 [42]. We recently conducted an
616 extensive analyses to understand if a 313 bp minibarcode is able to provide similar identifications
617 and species delimitations as the 658 bp barcodes and found this to be the case when examining
618 >5000 species [43]. Tagged primers were used for the PCRs as specified in Wang et al. (2018)
619 [44]. The PCR mix was as follows: 4 µl Mastermix from CWBio, 1µl of 1 mg/ml BSA, 1µl of 10 µM
620 of each primer, and 1ul of DNA. PCR conditions: 5 min initial denaturation at 94°C followed by 35
621 cycles of denaturation at 94°C (1 min), 47°C (2 min), 72°C (1 min), followed by final extension of
622 72°C (5 min). The PCR products were pooled and sequenced along with thousands of other
623 specimens in a lane of HiSeq 2500 (250 bp PE sequencing). The data processing followed Wang
624 et al. (2018): paired end reads were merged using PEAR (v 0.9.6) [45], reads were demultiplexed
625 by an inhouse pipeline that looks for perfect tags while allowing for 2 bp mismatches in primer
626 sequence. For each sample, demultiplexed reads are merged to identify the most dominant
627 sequence, and a barcode is accepted only if this sequence is 5X as common as the next most
628 common sequence.

629 **5. Assessment of MinION barcodes and mOTU delimitations**

630 Both MinION and Illumina barcodes were subject to contamination check. For MinION barcodes
631 we used preliminary MAFFT barcodes given that this is the largest barcode set. Barcodes were
632 matched to GenBank using BLASTN and taxonomic classifications were assigned using
633 readsidentifier [46]. Any barcode with >95% match to a non-phorid sequence was excluded from
634 the dataset. Furthermore, if any barcode best matched to Bacteria, it was also excluded.

635

636 MinION barcodes were assessed by scripts provided in the miniBarcoder package
637 (`assess_corrected_barcodes.py` and `assess_uncorrected_barcodes.py`). For uncorrected
638 barcodes, this was done by aligning barcodes to reference Illumina barcodes using `dnadiff` [47].
639 For corrected barcodes (+AA), we used MAFFT to obtain pairwise alignments. This allowed us to
640 compare per base accuracy. Here we excluded those barcodes that had >3% difference between
641 MinION and Illumina barcodes. These are likely due to wet lab errors (<0.5% of specimens). Such
642 error is not entirely surprising given that the MinION and Illumina barcodes were generated using
643 different amplicons.

644 We were further interested in understanding how mOTU delimitation is affected by error
645 correction. Barcodes were aligned using MAFFT and MinION barcodes were further trimmed to
646 the 313 bp region of the Illumina barcode. mOTU delimitation was done at 2, 3, and 4% using
647 `SpeciesIdentifier` (objective clustering) [48]. mOTU richness was estimated and we furthermore
648 calculated match ratio between two sets of clusters [49]. Match ratio is given by $\frac{2N_{match}}{N_1+N_2}$.

649 **6. Morphological examination**

650 For morphological examination of the clustered specimens we used 100 randomly selected non-
651 singleton mOTUs delimited at 5% but also kept track of sub-clusters within the large mOTUs that
652 were splitting at 1-5%. This allowed for examination of closely related, but potentially distinct,
653 species. We were mostly interested in understanding if MinION barcodes were placing specimens
654 into mOTUs incorrectly and hence we examined if specimens were consistent morphologically in
655 each of these 5% clusters. The choice of 5% cluster may seem initially inconsistent with the choice
656 of 3% for mOTU delimitation for other analyses, but examination of all specimens within 5%
657 clusters allows for comparing multiple closely related 3% (or 1-5%) mOTUs. This often requires
658 genitalia preparations which will be carried out at a larger scale once more specimens have been

659 sequenced. In this study, the process is only illustrated for the newly described species for which
660 we illustrate how the haplotype network obtained with the median joining method in PopART (Fig.
661 7) [50] guides morphological examination of specimens for the new species, *Megaselia*
662 *sepsioides* sp. nov.. Specimens with conspicuously large haplotype differences were dissected in
663 order to rule out the presence of multiple closely related species. Differences in setation were
664 observed between the two distant haplotypes (UGC0012899 and UGC001224) and the main
665 cluster (UGC0003003, UGC0005864, UGC0005996, UGC0006224, UGC0012568,
666 UGC0012937, and UGC0012971) and are detailed in Fig. 6. It is deemed likely that with further
667 collection of specimens from this haplotype cluster, these now rather distinct differences will be
668 absorbed into a continuum of intraspecific variation. Specimen examination was done with a Leica
669 m80 and Leica M205 C stereo microscopes and the images were obtained with a Dun Inc.
670 Microscope Macrophotography system (Canon 7D chassis with 10X Mitutoyo lens). Photography
671 stacking was done with Zerene stacker. Specimens were cleared with clove oil and mounted on
672 slides in Canada balsam following the protocol of Disney [51].

673 **7. Species Richness estimation**

674 The most accurate set of barcodes were used for assessing the overall diversity of the barcoded
675 phorids. mOTU delimitation was based on SpeciesIdentifier [48]. The 3% mOTUs were used for
676 estimating species richness. Here we used EstimateS9 [52], and changed the diversity settings
677 to use the classical formula of Chao1 and Chao2. This is because coefficient of variation of the
678 abundance or incidence distribution was >0.5 .

679

680 **AVAILABILITY OF SOURCE CODE AND REQUIREMENTS**

- 681 • Project name: miniBarcoder
- 682 • Project home page: <https://github.com/asrivathsan/miniBarcoder>

- 683 • Operating system(s): Linux, MacOSX (for initial barcode calling)
- 684 • Programming language: Python
- 685 • Other requirements: MAFFT BARCODE: MAFFT, glsearch36, RACON BARCODE:
686 GraphMap, Racon, and amino acid correction: BioPython, MAFFT
- 687 • License: GNU GPL
- 688 • New scripts included: mb_parallel_consensus.py mb_parallel_demultiplex.py,
689 repool_by_plate.py
- 690 • Updated scripts: consolidate.py, bug fix in aacorreption.py

691 **AVAILABILITY OF SUPPORTING DATA AND MATERIALS**

692 Besides the source code, the nanopore data and input files and barcode sets will be made
693 available once FTP link is obtained.

694 **DECLARATIONS**

695 **Competing Interests:** The author(s) declare(s) that they have no competing interests.

696 **Funding:** We would like to acknowledge support from the following grants: MOE grant for
697 biodiversity discovery (R-154-000-A22-112), NUS SEABIG grant (R-154-000-648-646 and R-
698 154-000-648-733), and institutional research funding (IUT21-1) of the Estonian Ministry of
699 Education and Research for O.K..

700 **Author's Contributions:** R.M. and A.S. conceived the workflow and the analytical approach.
701 O.K. conducted/organized the sampling and Diptera sorting and commented on the manuscript.
702 Molecular work was conducted by J.P., W.T.L., S.N.K., E.H..and A.S. Pipeline development and
703 data analyses was conducted by A.S. Morphological examination, and species description was
704 conducted by E.H. Figures were prepared by E.H., S.N.K., A.S. Manuscript was written by R.M.,
705 A.S. and E.H..

706 **Acknowledgements:** The material in Kibale National Park in Uganda was collected and
707 transferred in accordance with approvals from the Uganda Wildlife Authority (UWA/FOD/33/02)
708 and Uganda National Council for Science and Technology (NS 290/ September 8, 2011),
709 respectively. Yuchen Ang is thanked for his help photographing the new species and for his
710 suggestion of sepsioides as the specific epithet. Henry Disney and Brian Brown are thanked for
711 their consultation on the new species of *Megaselia*. We thank Arina Adom for help in curating the
712 Illumina barcodes and Sabrina Tang for help with photography.

713

714 REFERENCES

- 715 1. Wilson EO. Biodiversity research requires more boots on the ground. *Nat Ecol Evol.*
716 2017;1 11:1590-1. doi:10.1038/s41559-017-0360-y.
- 717 2. Krell F-T. Parataxonomy vs. taxonomy in biodiversity studies – pitfalls and applicability of
718 ‘morphospecies’ sorting. *Biodiversity and Conservation.* 2004;13 4:795-812.
719 doi:10.1023/b:Bioc.0000011727.53780.63.
- 720 3. Hebert PD, Cywinska A, Ball SL and deWaard JR. Biological identifications through DNA
721 barcodes. *Proceedings of Royal Society B.* 2003;270 1512:313-21.
- 722 4. Wang WY, Srivathsan A, Foo M, Yamane SK and Meier R. Sorting specimen-rich
723 invertebrate samples with cost-effective NGS barcodes: Validating a reverse workflow
724 for specimen processing. *Molecular Ecology Resources.* 2018;18 3:490-501.
- 725 5. Meier R, Wong W, Srivathsan A and Foo M. \$1 DNA barcodes for reconstructing
726 complex phenomes and finding rare species in specimen-rich samples. *Cladistics.*
727 2016;32 1:100-10.
- 728 6. Yeo D, Puniamoorthy J, Ngiam RWJ and Meier R. Towards holomorphology in
729 entomology: rapid and cost-effective adult–larva matching using NGS barcodes.
730 *Systematic Entomology.* 2018;43 4:678-91.

- 731 7. Hebert PDN, Braukmann TWA, Prosser SWJ, Ratnasingham S, deWaard JR, Ivanova
732 NV, et al. A Sequel to Sanger: amplicon sequencing that scales. *BMC Genomics*.
733 2018;19:219.
- 734 8. Shokralla S, Porter TM, Gibson JF, Dobosz R, Janzen DH, Hallwachs W, et al.
735 Massively parallel multiplex DNA sequencing for specimen identification using an
736 Illumina MiSeq platform. *Scientific Reports*. 2015;5:9687.
- 737 9. Creedy TJ, Norman H, Tang CQ, Chim KQ, Andujar C, Arribas P, et al. A validated
738 workflow for rapid taxonomic assignment and monitoring of a national fauna of bees
739 (Apiformes) using high throughput barcoding. *BioRxiv*. 2019; doi:10.1101/575308.
- 740 10. Krehenwinkel H, Kennedy SR, Rueda A, Lam A and Gillespie RG. Scaling up DNA
741 barcoding – Primer sets for simple and cost efficient arthropod systematics by multiplex
742 PCR and Illumina amplicon sequencing. 9. 2018;11 2181-2193.
- 743 11. Krehenwinkel H, Pomerantz A, Henderson JB, Kennedy SR, Lim JY, Swamy V, et al.
744 Nanopore sequencing of long ribosomal DNA amplicons enables portable and simple
745 biodiversity assessments with high phylogenetic resolution across broad taxonomic
746 scale. *GigaScience*. 2019; doi:10.1093/gigascience/giz006.
- 747 12. Krehenwinkel H, Wolf M, Lim JY, Rominger AJ, Simison WB and Gillespie RG.
748 Estimating and mitigating amplification bias in qualitative and quantitative arthropod
749 metabarcoding. *Scientific Reports*. 2017;7 17668.
- 750 13. Srivathsan A, Baloglu B, Wang W, Tan WX, Bertrand D, Ng AHQ, et al. A MinION™-
751 based pipeline for fast and cost-effective DNA barcoding. *Molecular Ecology Resources*.
752 2018;18 5:1035-49.
- 753 14. Brown BV: Phorid Catalog. <http://phorid.net/pcat/>. Accessed 27 April 2019.
- 754 15. Stork NE. How Many Species of Insects and Other Terrestrial Arthropods Are There on
755 Earth? *Annu Rev Entomol*. 2018;63:31-45. doi:10.1146/annurev-ento-020117-043348.

- 756 16. Zhang ZQ. Animal biodiversity: An introduction to higher-level classification and
757 taxonomic richness. Magnolia Press; 2011.
- 758 17. Forbes AA, Bagley RK, Beer MA, Hippee AC and Widmayer HA. Quantifying the
759 unquantifiable: why Hymenoptera – not Coleoptera – is the most speciose animal order.
760 BMC Ecology. 2018;18 21 doi:10.1101/274431.
- 761 18. Hebert PD, Ratnasingham S, Zakharov EV, Telfer AC, Levesque-Beaudin V, Milton MA,
762 et al. Counting animal species with DNA barcodes: Canadian insects. Philos Trans R
763 Soc Lond B Biol Sci. 2016;371 1702 doi:10.1098/rstb.2015.0333.
- 764 19. Borkent ART, Brown BV, Adler PH, Amorim DDS, Barber K, Bickel D, et al. Remarkable
765 fly (Diptera) diversity in a patch of Costa Rican cloud forest: Why inventory is a vital
766 science. Zootaxa. 2018;4402 1 doi:10.11646/zootaxa.4402.1.3.
- 767 20. Brown BV, Borkent A, Adler PH, De Souza Amorim D, Barber K, Bickel D, et al.
768 Comprehensive inventory of true flies (Diptera) at a tropical site. Communications
769 Biology. 2018;1 21:8. doi:10.1038/s42003-018-0022-x.
- 770 21. Marshall SA. Flies: The Natural History and Diversity of Diptera. Buffalo, New York:
771 Firefly Books; 2012.
- 772 22. Brown BV and Hartop EA. Big data from tiny flies: patterns revealed from over 42,000
773 phorid flies (Insecta: Diptera: Phoridae) collected over one year in Los Angeles,
774 California, USA. Urban Ecosystems. 2016; doi:10.1007/s11252-016-0612-7.
- 775 23. Vaser R, Sovic I, Nagarajan N and Sikic M. Fast and accurate de novo genome
776 assembly from long uncorrected reads. Genome Res. 2017;27 5:737-46.
777 doi:10.1101/gr.214270.116.
- 778 24. Kwong S, Srivathsan A, Vaidya G and Meier R. Is the COI barcoding gene involved in
779 speciation through intergenomic conflict?. Molecular Phylogenetics and Evolution.
780 2012;62 3:1009.

- 781 25. Hartop EA and Brown BV. The tip of the iceberg: a distinctive new spotted-wing
782 *Megaselia* species (Diptera: Phoridae) from a tropical cloud forest survey and a new,
783 streamlined method for *Megaselia* descriptions. Biodiversity Data Journal. 2014;2:e4093.
784 doi:10.3897/BDJ.2.e4093.
- 785 26. Hartop EA, Brown BV and Disney RHL. Opportunity in our ignorance: urban biodiversity
786 study reveals 30 new species and one new Nearctic record for *Megaselia* (Diptera:
787 Phoridae) in Los Angeles (California, USA). Zootaxa. 2015;3941:451-84.
- 788 27. Hartop EA, Brown BV and Disney RHL. Flies from L.A., The Sequel: Twelve further new
789 species of *Megaselia* (Diptera: Phoridae) from the BioSCAN Project in Los Angeles
790 (California, USA). Biodiversity Data Journal. 2016, p. e7756.
- 791 28. Riedel A, Sagata K, Surbakti S, Rene T and Michael B. One hundred and one new
792 species of *Trigonopterus* weevils from New Guinea. Zookeys. 2013; 280:1-150.
793 doi:10.3897/zookeys.280.3906.
- 794 29. ONT: <https://store.nanoporetech.com/kits-250/1d-sequencing-kit.html>. Accessed 28 April
795 2019.
- 796 30. Erwin TL. Tropical Forests: Their Richness in Coleoptera and Other Arthropod Species.
797 The Coleopterists Bulletin. 1982;36 1:74-5.
- 798 31. Longino JT, Coddington J and Colwell RK. The ant fauna of a tropical rain forest:
799 estimating species richness three different ways. Ecology. 2002;83:689-702.
- 800 32. Townes H. A light-weight Malaise trap. Entomological News. 1972;83:239-47.
- 801 33. Howard PC. Nature conservation in Uganda's tropical forest reserves. The IUCN
802 Tropical Forest Programme. 1991.
- 803 34. Chapman CA and Chapman LJ. Forest regeneration in logged and unlogged forests of
804 Kibale National Park, Uganda. Biotropica. 1997;29:396-412.
- 805 35. Kurina O. Description of four new species of *Zygomomyia* Winnertz from Ethiopia and
806 Uganda (Diptera: Mycetophilidae). African Invertebrates. 2012;53 1:205-20.

- 807 36. Folmer O, Black M, Hoeh W, Lutz R and Vrijenhoek R. DNA primers for amplification of
808 mitochondrial cytochrome c oxidase subunit I from diverse metazoan invertebrates.
809 *Molecular Marine Biology and Technology*. 1994;3 5:294-9.
- 810 37. Comai L and Howell T. Barcode Generator.
811 http://comailabgenomecenter.ucdavis.edu/index.php/Barcode_generator. 2012.
- 812 38. Katoh K and Standley DM. MAFFT multiple sequence alignment software version 7:
813 improvements in performance and usability. *Molecular Biology and Evolution*. 2013;30
814 4:772-80.
- 815 39. Sovic I, Sikic M, Wilm A, Fenlon SN, Chen S and Nagarajan N. Fast and sensitive
816 mapping of nanopore sequencing reads with GraphMap. *Nature Communications*.
817 2016;7:11307.
- 818 40. Vaser R, Sovic I, Nagarajan N and Sikic M. Fast and accurate de novo genome
819 assembly from long uncorrected reads. *Genome Research*. 2017;27 5:737-46.
- 820 41. Leray M, Yang JY, Meyer CP, Mills SC, Agudelo N, Ranwez V, et al. A new versatile
821 primer set targeting a short fragment of the mitochondrial COI region for metabarcoding
822 metazoan diversity: application for characterizing coral reef fish gut contents. *Frontiers in*
823 *Zoology*. 2013;10:34.
- 824 42. Geller JM, C., Parker M and Hawk H. Redesign of PCR primers for mitochondrial
825 cytochrome c oxidase subunit I for marine invertebrates and application in all-taxa biotic
826 surveys. *Molecular Ecology Resources*. 2013;13 5:851-61.
- 827 43. Yeo D, Srivathsan A and Meier R. Mini-barcodes are more suitable for large-scale
828 species discovery in Metazoa than full-length barcodes. *bioRxiv*. 2019.
829 doi:10.1101/594952.
- 830 44. Wang WY, Srivathsan A, Foo M, Yamane SK and Meier R. Sorting specimen-rich
831 invertebrate samples with cost-effective NGS barcodes: Validating a reverse workflow

832 for specimen processing. *Molecular ecology resources*. 2018;18 3:490-501.
833 doi:10.1111/1755-0998.12751.

834 45. Zhang J, Kobert K, Flouri T and Stamatakis A. PEAR: a fast and accurate Illumina
835 Paired-End reAd mergeR. *Bioinformatics*. 2014;30 5:614-20.

836 46. Srivathsan A, Sha JC, Vogler AP and Meier R. Comparing the effectiveness of
837 metagenomics and metabarcoding for diet analysis of a leaf-feeding monkey (*Pygathrix*
838 *nemaeus*). *Mol Ecol Resour*. 2015;15 2:250-61. doi:10.1111/1755-0998.12302.

839 47. Kurtz S, Phillippy A, Delcher AL, Smoot M, Shumway M, Antonescu C, et al. Versatile
840 and open software for comparing large genomes. *Genome biology*. 2004;5 2:R12.
841 doi:10.1186/gb-2004-5-2-r12.

842 48. Meier R, Shiyang K, Vaidya G and Ng PKL. DNA Barcoding and Taxonomy in Diptera: A
843 Tale of High Intraspecific Variability and Low Identification Success. *Systematic Biology*.
844 2006;55 5:715–28.

845 49. Ahrens D, Fujisawa T, Krammer HJ, Eberle J, Fabrizi S and Vogler AP. Rarity and
846 Incomplete Sampling in DNA-based Species Delimitation. *Systematic Biology*. 2016;65
847 3:478-94.

848 50. Leigh JW and Bryant D. PopART: Full-feature software for haplotype network
849 construction. *Methods Ecol Evol*. 2015;6 9:1110-6.

850 51. Disney RHL. Scuttle flies (Diptera: Phoridae) Part II: the genus *Megaselia*. *Fauna of*
851 *Arabia*. 2009;24:249-357.

852 52. Colwell RK. EstimateS: Statistical estimation of species richness and shared species
853 from samples. Version 9 and earlier. User's Guide and application. 2013.
854
855

856 **Figure Legends**

857 **Figure 1:** Flowchart for generating MinION barcodes.

858 **Figure 2:** Effect of re-pooling on coverage of barcodes for both sets of specimens.

859 **Figure 3:** Ambiguities in MAFFT+AA (Purple), RACON+AA (Yellow) and Consolidated barcodes
860 (Green) with varying namino parameters (1,2 and 3). One outlier value for Racon+3AA barcode
861 corresponding to 13% ambiguities was excluded from the plot.

862 **Figure 4:** The Malaise trap that revealed the estimated >1000 mOTUs as shown by the species
863 richness estimation curve. Green: Chao1 Mean, Pink: S (Mean), Orange: Singleton Mean, Purple:
864 Doubleton mean.

865 **Figure 5:** Lateral habitus (a) and diagnostic features of *Megaselia sepsioides* spec. nov. (a,
866 inset) terminalia, (b) posterior view of foreleg, (c) anterior view of midleg (d,e) anterior and
867 postero-dorsal views of hindleg, (e) dorsal view of thorax and abdomen.

868 **Figure 6:** Haplotype variation of *Megaselia sepsioides* spec. nov. (a) UGC0005996, (b)
869 UGC0012244, (c) UGC0012899. UGC numbers refer to specimen IDs.

870 **Figure 7:** Haplotype network for *Megaselia sepsioides* spec. nov. UGC numbers refer to
871 specimen IDs.

Table 1: Number of reads and barcodes generated via MinION sequencing.

	Set 1: Two flowcells	Set 2: One flowcell	Combined (set 1 & 2)*
# Specimens	4275	4519	8699
Resequencing (re-pooled)	2172	2211	
# reads/# reads >600 bp	7,035,075/3,703,712	7,179,121/2,652,657	NA
Initial sequencing (all)	3,069,048/1,942,212	4,853,363/2,250,591	
Resequencing (re-pooled)	3,966,027/1,761,500	2,325,758/402,066	
# demultiplexed reads	898,979 (24.3%)	647,152 (24.4%)	
Initial sequencing (all)	562,434 (29%)	561,383 (24.9%)	
Resequencing (re-pooled)	336,545 (19%)	85,769 (21.3%)	
Combined results of original and resequencing runs			
# specimens with >=5X coverage	4227 (98.9%)	4287 (94.9%)	8428 (96.9%)
# MAFFT barcodes <1% N's	3797 (88.8%)	3476 (76.9%)	7220 (83%)
# MAFFT + AA barcodes	3774 (88.3%)	3464 (75.7%)	7178 (82.5%)
# RACON barcodes	3797 (88.8%)	3476 (76.9%)	7220 (83%)
# RACON +AA barcodes	3790 (88.7%)	3469 (76.7%)	7194 (83%)
# Consolidated barcodes	3740 (87.4%)	3394 (75%)	7115 (81.8%)
# Consolidated barcodes (non-phorids removed)	3700 (86.7%)	3369 (74.6%)	7062 (81.2%)
# mOTUS (2/3/4%)			728/685/636

* one plate was accidentally sequenced in both runs, wherever duplicates were present, second run was selected.

Table 2. Accuracy of MinION as assessed by Illumina barcodes. The overall optimal strategy is “Consolidated (namino=2)”. Optimal congruence values are highlighted in green.

Dataset	# compared with Illumina	Accuracy	# barcodes with errors/# >3% errors	mOTU richness deviation between MinION and Illumina barcodes		
				2%	3%	4%
MAFFT	6330	99.6091	4473/31	-3 (-0.43%)	-1 (-0.15)	-8 (-1.3)
RACON	6330	99.5075	4526/37	15 (2.08%)	5 (0.75)	-3 (-0.48)
MAFFT + AA (namino=1)	6146	99.9689	269/30	-6 (-0.85%)	-4 (-0.61)	-15 (-2.7)
MAFFT + AA (namino=2)	6146	99.9795	218/28	-8 (-1.15%)	-6 (-0.91)	-13 (-2.2)
MAFFT + AA (namino=3)	6286	99.967	350/28	-7 (-0.1%)	-4 (-0.61)	-14 (-2.2)
RACON + AA (namino=1)	6319	99.9617	419/27	5 (0.72%)	1 (0.15)	-3 (-0.48)
RACON + AA (namino=2)	6319	99.9711	326/27	2 (0.29%)	-2 (-0.31)	-5 (-0.81)
RACON + AA (namino=3)	6319	99.9664	383/29	4 (0.57%)	-2 (-0.3)	-8 (-1.28)
Consolidated (namino=1)	6230	99.9855	191/25	-1 (-0.14%)	-2 (-0.30)	-3 (-0.48)
Consolidated (namino=2)	6255	99.9864	185/25	0 (0%)	-3 (-0.45)	-4 (-0.64)
Consolidated (namino=3)	6250	99.9762	329/26	1 (0.14%)	-1 (-0.15)	-4 (-0.48)

WETLAB PROCEDURE

Fig. 1

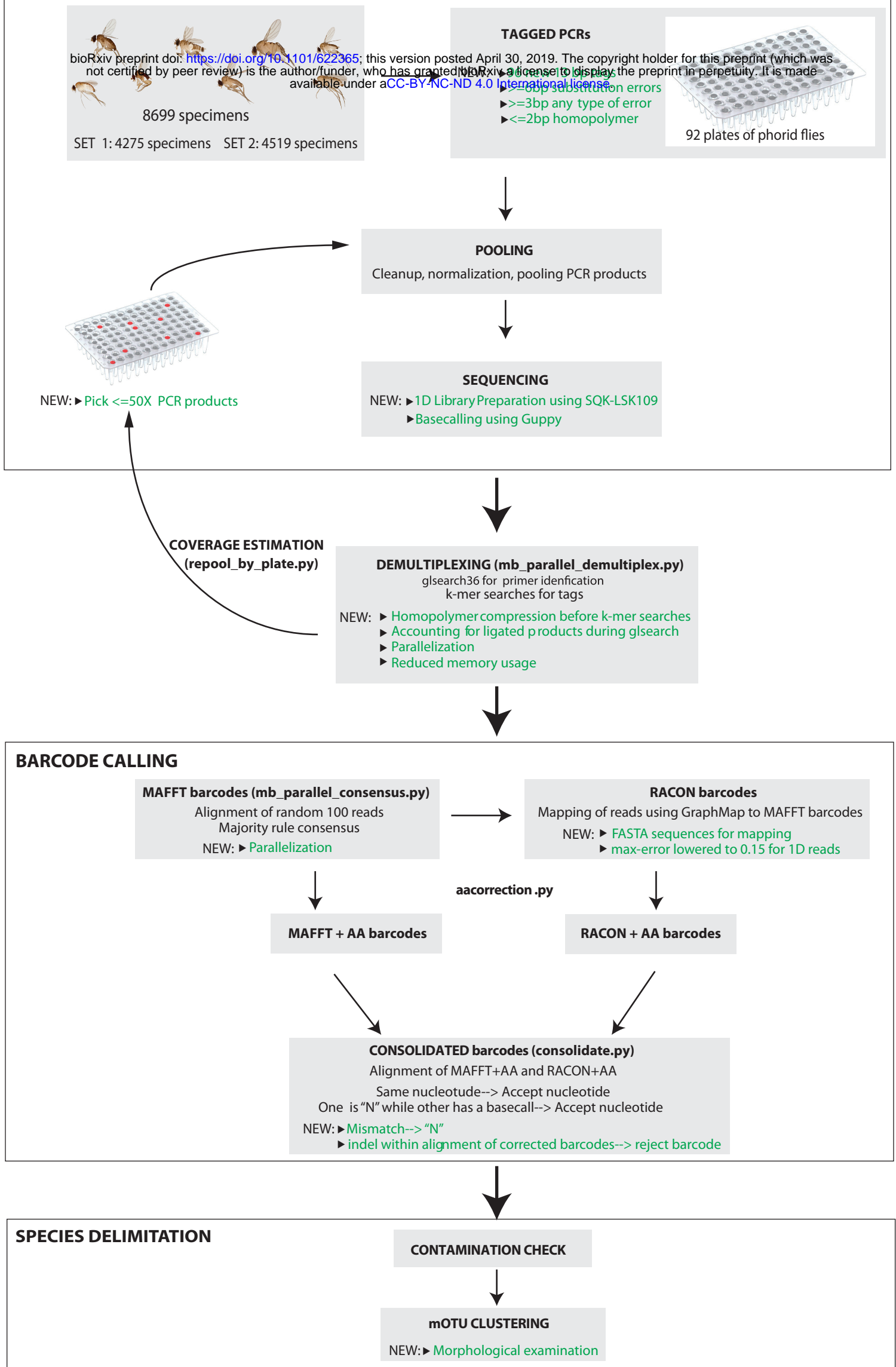


Fig. 2

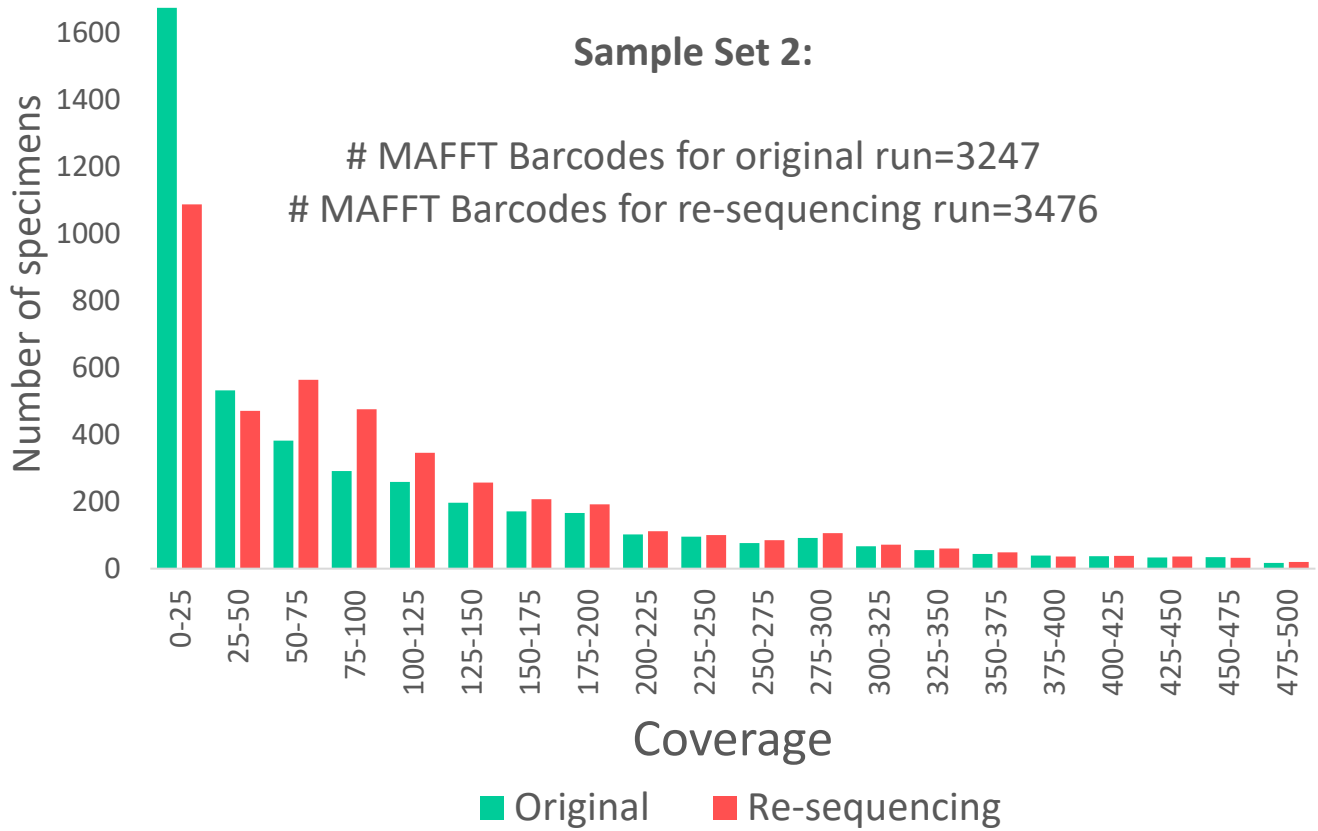
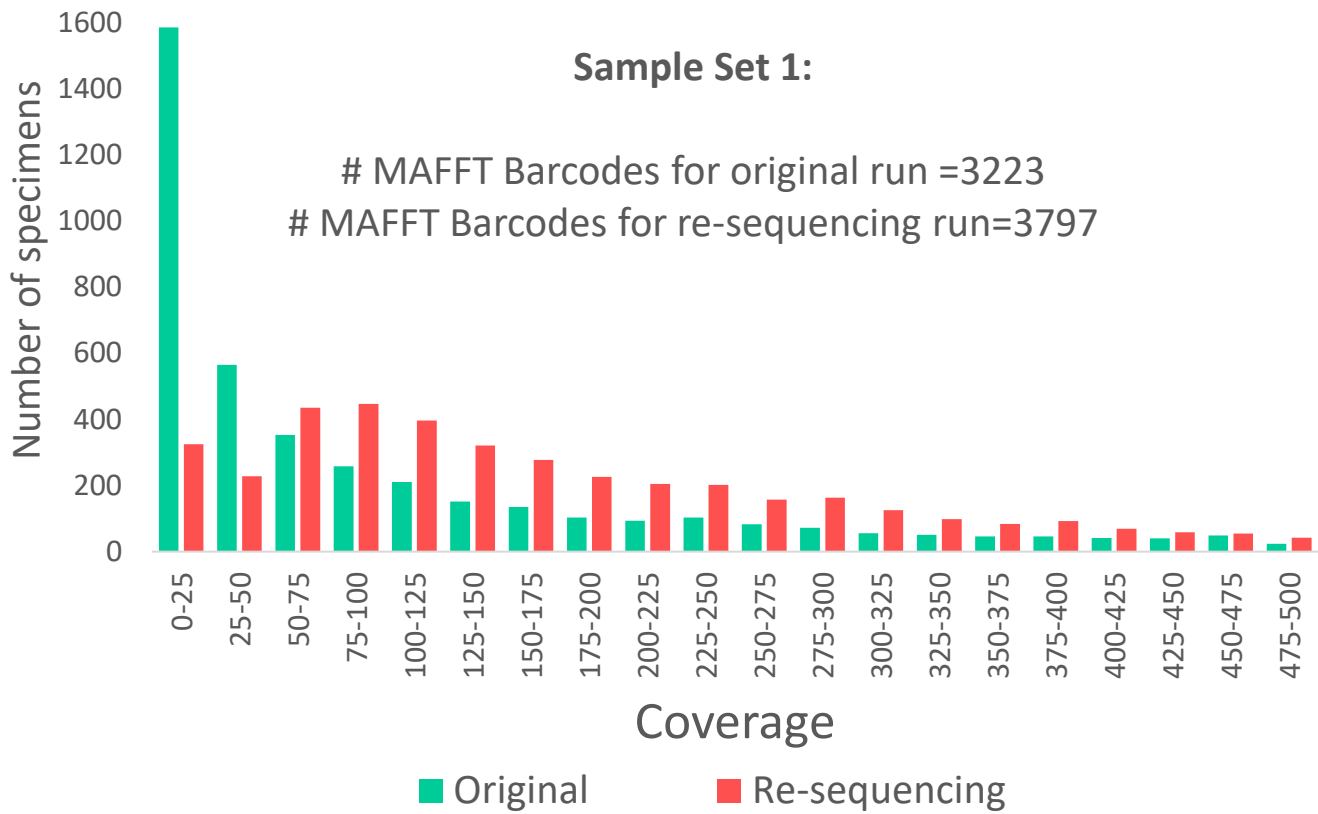


Fig. 3

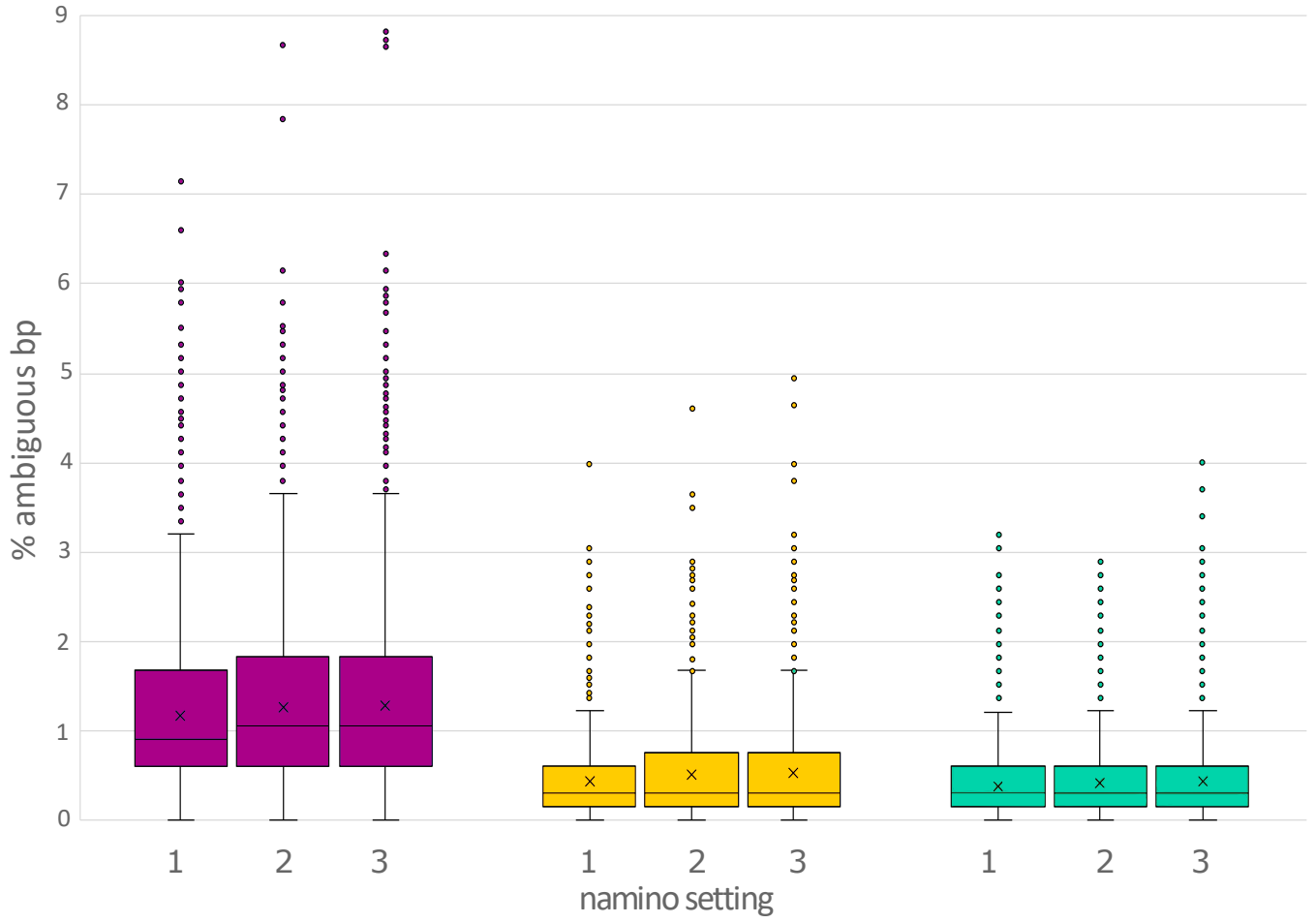


Fig. 4

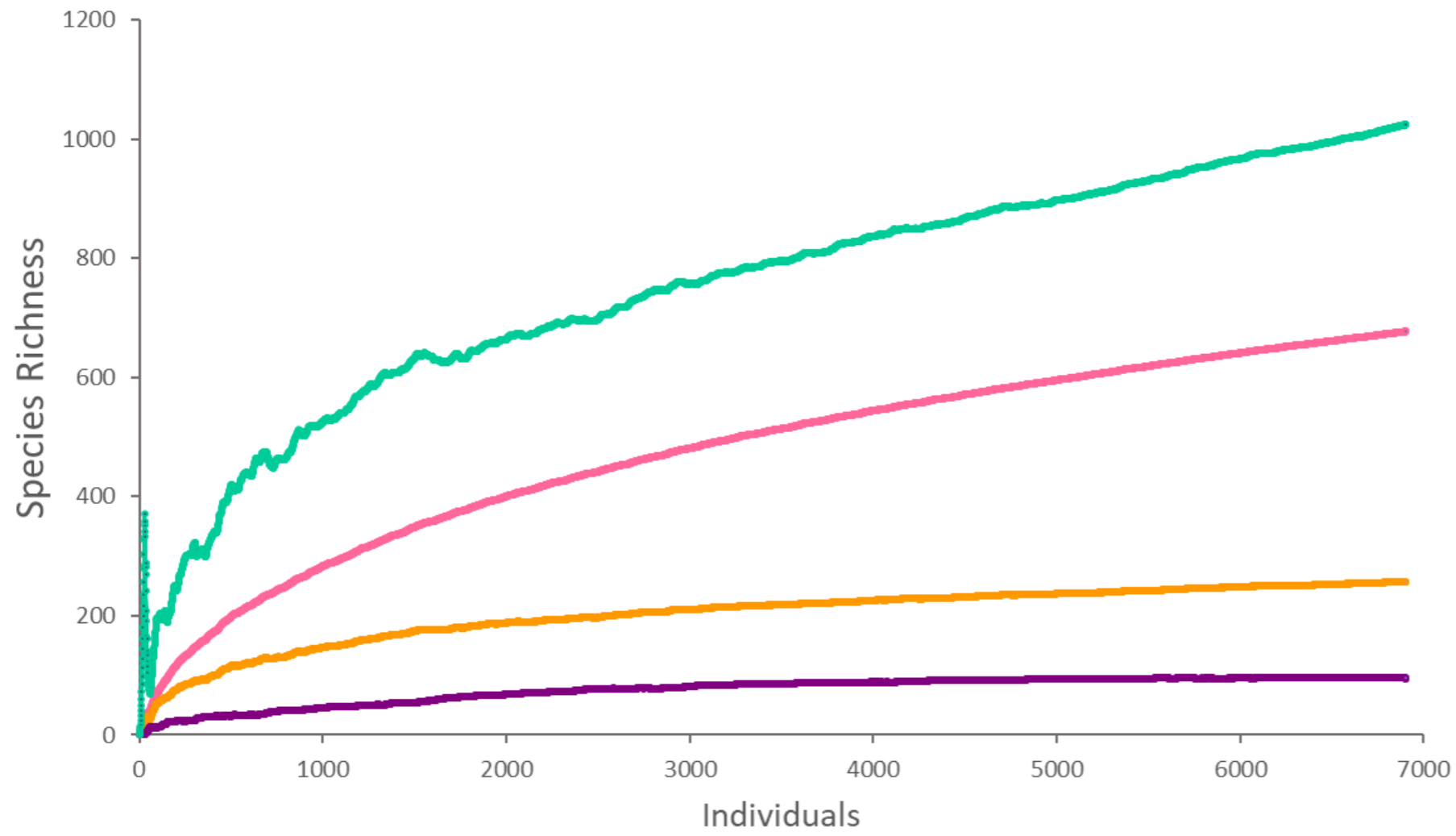


Fig. 5



a



b

c

d

e

f



a



b



c

Fig. 7

